Key Engineering Materials
ISSN: 1662-9795, Vol. 926, pp 1303-1316
doi:10.4028/p-f0d0u9

Submitted: 2021-12-08
Revised: 2022-02-03
Accepted: 2022-02-18
Online: 2022-07-22

Robotic-Assisted Measurement of Fabrics for the Characterization of the Shear Tension Coupling

Langat K. Rogers[1,2,a], De Luycker Emmanuel[1,b*], Noureddine Farid[1,c], and Rakotondrabe Micky[1,d]

[1]Laboratoire Génie de Production, LGP, Université de Toulouse, INP-ENIT, Tarbes, France

[2]Dedan Kimathi University of Technology, Nyeri, Kenya

[a]rogers.langat@enit.fr, [b]emmanuel.de-luycker@enit.fr, [c]farid.noureddine@enit.fr, [d]micky.rakotondrabe@enit.fr

Keywords: Hyperelasticity, Composites, Shear-Tension, Fabric, Textiles, Robotics, Characterization.

Abstract. Industrial use of composite materials requires an increasingly advanced knowledge of technical textiles' mechanical properties to control the manufacturing process and guarantee the performances of the finished products. Among the qualities that influence greatly the shaping process, the shear deformability is key for the forming of complex composite parts with double curves geometries. On the other hand, the stiffening of the behavior as the shearing rise is responsible for the occurrence of the wrinkling defect. This shearing behavior of the textile reinforcement is difficult to determine because it is non-linear and it coexists with a tensile stiffness of the fibers that is several orders of magnitude higher. Furthermore, shear and tension are coupled due to the weaving of the textiles. Now, few experimental methods have been proposed to measure the tension behavior of fabric as a function of its shear level because dedicated devices are needed for this investigation, capturing the shear-tension coupled behavior of fabric is then a difficult task. This paper deals with the robotization of the fabric shear-tension effect characterization. A KUKA robot associated with a force/torque sensor is utilized, taking advantage of its benefits in the ability to control the state of yarn tensions during shear tests while keeping track of the desired trajectory as enabled by the hybrid position-force control feature. This ensures precise positioning of a sample fabric and accurate contact forces. An anisotropic hyperelastic constitutive model for fabrics, based on the continuum theory of mechanics that takes into account the shear-tension coupling effect was formulated analytically and numerically simulated using Matlab software. An experimental test was then implemented to validate the proposed model. The results from a uni-axial tensile test and shear test under constant uni-axial tensile loading were obtained and analyzed to characterize the test sample. The model parameter identification was performed and presented in detail.

Introduction

The use of technical textiles in manufacturing composite reinforced products has immensely risen with great interest being registered in a wide range of industrial sectors such as automotive, aeronautical, defense, sports, and energy production [1, 2, 3]. This recognition is thanks to their promising specific mechanical performances and great advantages with regards to the strength-to-weight ratio [4]. They also offer resistance to fatigue and corrosion attack. Moreover, with the use of technical textiles in manufacturing, complex shapes that are not developable can be obtained by a single forming operation [5]. Indeed, a combination of all these advantages has led to a paradigm shift in the industrial application of fabric composites as researchers and industries seek to develop composites products with greater performances and a wide range of applicability all to meet the thresholds for customer satisfaction in connection to the product's reliability.

To optimize the usage of these materials, complete mastery of their mechanical behavior is necessary. This has not yet been fully acquired, which somehow compromises their application for composites in the rising high-tech industries with a key interest in technical textiles. Therefore, it is important

to investigate the properties that greatly influence the shaping process of the fabrics when forming a composite product [6]. This is because, during the forming process of technical textile composites, there is an occurrence of relative fiber motion which consequentially creates a mechanical behavior that characterizes low rigidities [5]. This creates room for wrinkles development in the preform [7], which may grow and extend to the useful part of the preform [6, 8]. In order to obtain, for instance, a double-curved-shaped preform, large in-plane shear may be needed, which in some cases, leads to the folding of the preform due to yarn overlaps [5] which results in double-curve shaped products with defects / fractures. This thus compromises the desired mechanical properties of the formed product as it becomes susceptible to impact damages. In fact, prediction of the occurrence of these folds and wrinkles during forming can be achieved through proper characterization of the technical textile's behavior in determining their mechanical properties which aids in avoidance of defects in manufactured products. Researchers continue to study and investigate these materials towards the development of models that defines the forming process, however, at present the available material models needs further improvement to exhaustively predict the forming of technical textiles [9, 10, 11]. This calls for further characterization and development of reliable models to define proper manufacturing parameters that guarantee the desired quality of the finished products.

The textiles are made of interlaced yarns referred to as warp and weft, and the position of these yarns and the orientation of the fibers impact greatly on the mechanical properties of the composite structure formed from the technical textile [12]. Phillipe Boisse et al. [6] discussed the need to study the deformation pattern for defining proper tooling parameters i.e the punch speed and loading, in an effort to acquire a near-net-shape product avoiding undesirable deformation outcomes or excessive residual stresses argued by Koimeli and Milani [13]. As a matter of fact, fibers are not constrained together in dry fabrics and when subjected to loading, they tend to slide on each other causing low stiffness of yarns in all directions other than the axial tension [13]. Rotation of the yarns at the wove joints as the deformation occurs is witnessed and this property leads to a change in the angle between warp and weft, which is actually the main deformation mechanism occurring in the fabric forming process [14]. As a result of these angular variations in the fabric, large in-plane shear strains are registered. The shear stiffness is normally weak for small angles and becomes significant for large shear angles, more so when the shear-locking angle is attained and exceeded in deformation [15]. This mechanical property would normally lead to the formation of wrinkles as discussed in [16]. Werner et al. [17], in their review on the modeling of fabric coupling mechanisms commented on the shear stress characteristic during angular variation of the rovings. Immediately the yarns come into contact with each other, the shear force increases, which is definitely attributed to the lateral compaction of rovings. At the maximum state of compaction, any further deformation will call for large force applications. This in addition creates high compressive stresses across the fibers which lead to buckling effect due to the low bending stiffness of fabrics [6, 18].

Moreover, the tensile behavior is highly non-linear due to crimp inter-change (in essence the unfolding occurs) and the traverse crushing of the yarns which compresses it with normal frictional forces [5]. This non-linearity may be occurring as well from the lateral crushing between yarns which occurs when the shear angle becomes large [15]. Kashani et al.[19] presented an experimental investigation of the uni-axial stress-strain effect. From their work, it is indeed evident that strain in one fiber direction induces both longitudinal normal stresses and stresses in transverse directions. According to [17], the crimping in the rovings is reduced along the loaded direction. As this happens waviness of the unloaded yarn direction increases leading to the effect referred to as "crimp interchange". As this stage fades away due to further loading, yarns are stretched, which is then impacted by the high tensile stiffness that brings about a sharp increase in tensile stresses with increasing longitudinal strain [17, 19, 20, 21].

These very critical and complex mechanical properties have been studied independently while neglecting their coexistence and interaction. This explains the low confidence in the available models to correctly capture the onset of deformations in composite preforms [22]. Researchers have however responded to a call to develop reliable simulation models and experimental methods that take into

account the impactful effect of shear tension coupling in the accurate prediction of buckles [23]. Harrison et al. [22, 24] presented a very interesting experimental method that captures the shear tension coupling. The effort to characterize and well describe this effect has drawn the attention of researchers, Yao et al. [23] in their recent study, for instance, noted that it was really important to accurately obtain the material's coupling parameters more so when there is need to manufacture a part with curved surfaces. In addition, various models that have been proposed recently geared towards advancing the numerical simulations accuracy are based on the non-linear anisotropic hyperelastic constitutive models, following Spencer's continuum theory of mechanics. Fibers, in this case, are considered to be continuously distributed through the material, which on a macroscopic level, treat the concerned material as strongly anisotropic continuum material [25]. Based on this theory, many researchers [2, 15, 23, 26], have developed hyperelastic constitutive models to investigate the mechanical behaviour of dry fabrics under large deformations. Indeed, the non-linear macroscopic material behavior has to be set in the constitutive equations [17]. It is also worth noting that in the framework of in-plane shear tests, two major methods have been proposed and studied i.e Picture Frame Test and Bias Extension Test. The results from these methods have qualified them for reliability in the investigation of the shear forces evolution with the shear angles, fibers since it produces comparable results [27, 28]. Taha et al. [27] and Harrison et al. [28] made comparison of these two methods and established in their results that, Bias-extension test is fast and simple in setting up, however, data analysis from this method possess more challenges due to the interaction of the non-shear components. The picture frame test proved to be time-consuming yet its data analysis is way simpler as it offers a pure shear deformation throughout the sample in the test [29, 30, 31].

This paper introduces a new experimental method based on the use of robots in the characterization of textiles which offers precise control of forces; both in the magnitude of the loading and direction of application as well as the ability to control and obtain the intermediate positions in space (X, Y, and Z direction). The advancement of industrial application of robotics in the current industrial revolution has been attributed to the fact that they can be easily integrated with sensors and controllers which then enables the execution of control laws that guides in obtaining the desired trajectory. For the applications that involve material handling and testing, a planned trajectory is entrusted to the control system which should provide the robot's actuators with the commands consistent with the planned motion [32]. This advancement in control of robotics has created a huge community of parties interested in robotics since it facilitated the possibility to automate complex industrial tasks which could however be difficult to automate with traditional robot platforms as they had no room for sensor integration in the real-time control loop [33]. Therefore, by including the sensors in the control loop, there is a possibility to let the robot interact with the environment while in operation and be able to track the desired path. This flexibility makes it also possible to use the robot system not only for operations that are pre-programmed but where the products cannot be modeled satisfactorily, for example, due to non-rigid materials [33] as in the case of technical textiles testing process. It also goes ahead to extend the model proposed by Yao et al. [23], simple invariant based anisotropic constitutive hyperelastic model. In the same nature, it captures the shear-tension coupling effect. The formulated model was simulated to assess the coupling contribution in the fabric shear behavior and finally, an experimental benchmark was set using a KUKA robot associated with the ATI Multi-Axis Force/Torque Sensor (Delta IP60 Series). The obtained experimental data were analyzed and used to perform model identification by fitting the formulated constitutive model to the experimental tissue behavior. The material parameters for the tension, shear, and coupling behavior were deduced from the experimental data accordingly.

Materials and Methods

The material used in the experimental tests Fig. 1 is a balanced plain weave composed of 100 % flax fiber. The material specifications parameters are presented in Table 1. To run the characterization experiment a fabric piece of 100 mm by 200 mm was prepared. It is worth noting that the proposed model can be well utilized to characterize other textile materials in extension.

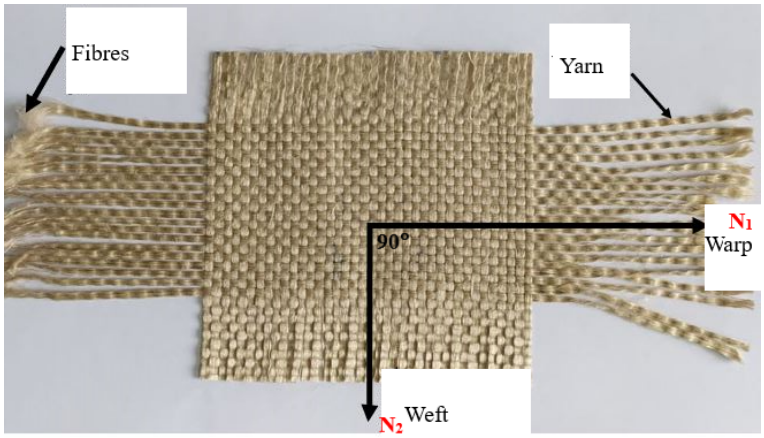

Fig. 1: The architecture of the test material.

Table 1: Characteristics of the material used to run tests.

Material Specifications					Sample Dimensions	
Weave	Material	Surface density	Warp density	Weft density	Warp length	Weft length
Plain	Desized-up flax	458 [g/m²]	380 [/m]	385 [/m]	200 [mm]	100 [mm]

Analytical Modeling. Working on the framework of hyperelasticity, an analytical model was constituted. From the work of [2, 15], the existence of potential energy (per undeformed unit volume) which is a function of a gradient strain tensor $\underline{\underline{F}}$ can be assumed, in which case this function must satisfy the principle of material indifference. The strain energy density function can be presented according to:

$$W = W(\underline{\underline{C}}) \qquad \text{where} \qquad \underline{\underline{C}} = \underline{\underline{F}}^T.\underline{\underline{F}} \tag{1}$$

This energy is influenced by the material fiber network directions and can be incorporated in the formulations using any scalar, vectorial, or tensorial functions relative to any anisotropy. Therefore, W must be mathematically isotropic as argued in [15], which by representations theorem, can be expressed using invariants with physical importance for woven fabric complex behavior. In our case, to model the mechanical behavior of the fabric, the choice of invariants was majorly dictated by the deformation modes, that is, tensile strain in warp and weft directions and the in-plane shear strain. The fabric under study is a balanced plain weave made of interlaced warp and weft yarns, with a representation of $\mathbf{N_1}$ and $\mathbf{N_2}$ vectors respectively, which are perpendicular to each other in the reference frame (initial configuration) shown in Fig. 1. Hence, W can be expressed as a scalar function of the related principal invariants I_i such as those presented in [23].

$$W = W(\underline{\underline{C}}, \underline{N}_1, \underline{N}_2) = W(I_i) \tag{2}$$

The invariants are: $I_1 = tr(\underline{\underline{C}}), I_2 = \frac{1}{2}[(tr\underline{\underline{C}})^2 - tr(\underline{\underline{C}})^2], I_3 = det(\underline{\underline{C}}), I_4 = \underline{N}_1 \cdot \underline{\underline{C}} \cdot \underline{N}_1 = \lambda^2_{\underline{N}_1}$,
$I_5 = \underline{N}_1 \cdot \underline{\underline{C}}^2 \cdot \underline{N}_1, I_6 = \underline{N}_1 \cdot \underline{\underline{C}} \cdot \underline{N}_2, I_7 = \underline{N}_1 \cdot \underline{\underline{C}}^2 \cdot \underline{N}_2, I_8 = \underline{N}_2 \cdot \underline{\underline{C}} \cdot \underline{N}_2 = \lambda^2{}_{\underline{N}_1}, I_9 = \underline{N}_2 \cdot \underline{\underline{C}}^2 \cdot \underline{N}_2$
Calculation of the structural tensors defining the fiber directions in initial coordinates follows:

$$\underline{\underline{N}}_{11} = \underline{N}_1 \otimes \underline{N}_1 \qquad \underline{\underline{N}}_{22} = \underline{N}_2 \otimes \underline{N}_2 \qquad \underline{\underline{N}}_{12} = \underline{N}_1 \otimes \underline{N}_2 \qquad \underline{\underline{N}}_{21} = \underline{N}_2 \otimes \underline{N}_1 \tag{3}$$

Inferring from [15], to compute the second kind of invariants with regards to the deformations, it follows:
Starting with the tensile deformation in the fiber directions, the warp stretch significant invariant is calculated according to:

$$I_{41} = \underline{\underline{N}}_{11} \cdot \underline{\underline{C}} \cdot \underline{\underline{N}}_{11} \text{ Consequently, the second type invariant becomes: } I2(1) = \frac{log(I_{41})}{2} \quad (4)$$

A similar case applies in the weft direction:

$$I_{42} = \underline{\underline{N}}_{22} \cdot \underline{\underline{C}} \cdot \underline{\underline{N}}_{22} \text{ resulting in : } I2(2) = \frac{log(I_{42})}{2} \quad (5)$$

The invariant resulting from the shear deformation can be computed according to:

$$I_{412} = \underline{\underline{N}}_{12} \cdot \underline{\underline{C}} \cdot \underline{\underline{N}}_{12} \text{ and the second type invariant becomes: } I2(3) = \frac{I_{412}}{\sqrt{I_{41} \cdot I_{42}}} = sin(\gamma) = I_{sh} \quad (6)$$

The tensile deformation results in two energies in the warp and weft directions due to the stretch elongations, the tension energy is thus given by:

$$W_{Tension} = W_{warp} + W_{weft} = W_{Tension} = \sum_{i=1}^{4} T_i [I_{4\alpha} - 1]^i \quad (7)$$

where T_i represents the tension parameters.
On the other hand, from the shear invariant, we can deduce the shear energy potential from:

$$W_{shear} = S_1 \cdot I_{sh}^2 + S_2 \cdot I_{sh}^4 + S_3 \cdot I_{sh}^6 + S_4 \cdot I_{sh}^8 + S_5 \cdot I_{sh}^{10} \quad (8)$$

where S_i represents the shear parameters.
Focusing on the shear potential, in consideration of the coupling effect, the potential with shear-tension relationship provided by [23] is presented as:

$$W_{shear}(I_{41}, I_{42}, I_{sh}) = \sum_{i=1}^{5} S_i (I_{sh})^i + \sum_{i=1}^{2} c_i I_{sh}^2 [I_{4\alpha} - 1]^i \quad (9)$$

where $\alpha = 1, 2$.
Expanding Eq. 9, we have the coupled shear potential as:

$$W_{shear} = S_1 I_{sh}^2 + S_2 I_{sh}^4 + S_3 I_{sh}^6 + S_4 I_{sh}^8 + S_5 I_{sh}^{10} + c_1 I_{sh}^2 [I_{4\alpha} - 1]^2 + c_2 I_{sh}^2 [I_{4\alpha} - 1]^4 \quad (10)$$

where c_i represents the coupling parameters.

Numerical Modeling. To validate the proposed model in Eq. 10, a numerical model was implemented using a unit square sample. This was set to answer the question on the effect of the tension-shear coupling on the fabric's complex mechanical behavior. The elementary deformation modes were simulated and analyzed to deduce their significant characteristics. The uni-axial tensile load was applied while recording and saving the longitudinal elongation values in the warp direction, after which, a shear deformation with pre-tensioned yarns was explored. This can be well visualized from Fig. 2a, 2b, and 2c. The angular variations in the fiber direction were recorded.
From the simulation data, significant invariants and strain energies concerning the deformation modes were computed and plotted to compare the two cases. That is tension-Shear strain energy with and without coupling.

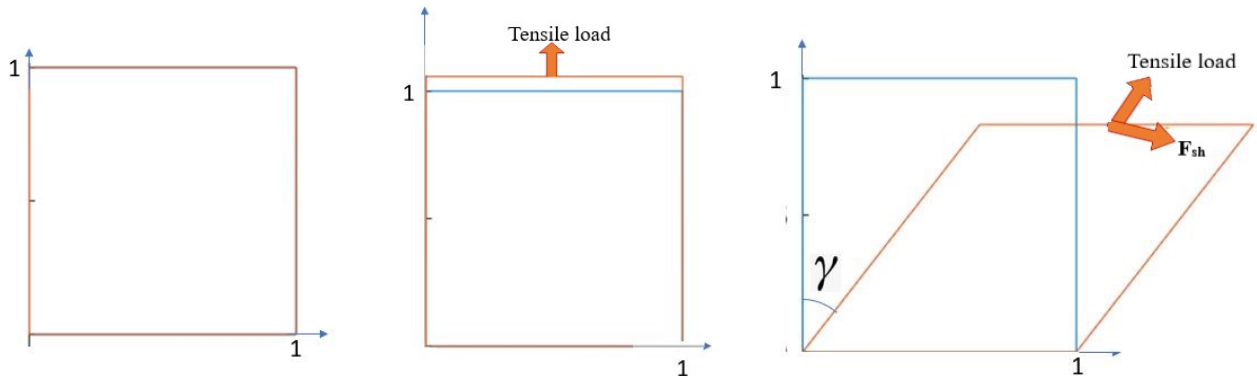

Initial configuration. Tensile deformation mode. Coupled shear deformation mode.

Fig. 2: Simulated Elementary Deformation Modes.

Experimental Procedure. In the experimental setup, a KUKA robot with a KR C4 controller was used. This robot had already been integrated with an ATI Delta IP60 multi-axis force/torque (F/T) sensor. This enhances control in cases where contact control is desired. Accordingly, to utilize this KUKA robot, a control and path planning program was generated and executed. Using the KUKA teach pendant (KTP), points were defined on the trajectory that the robot end-effector had to follow during the test process. Moreover, since both position and contact forces were of great concern in our research, the KUKA force-torque control algorithm was implemented to enable the execution of motion as a function of the applied forces, thanks to the KUKA robot sensor interface (RSI). A textile gripper mount similar to the picture frame test equipment, shown in the central image of Fig. 3, was fabricated and installed on the robot platform. The whole experimental benchmark is displayed in Fig. 3.

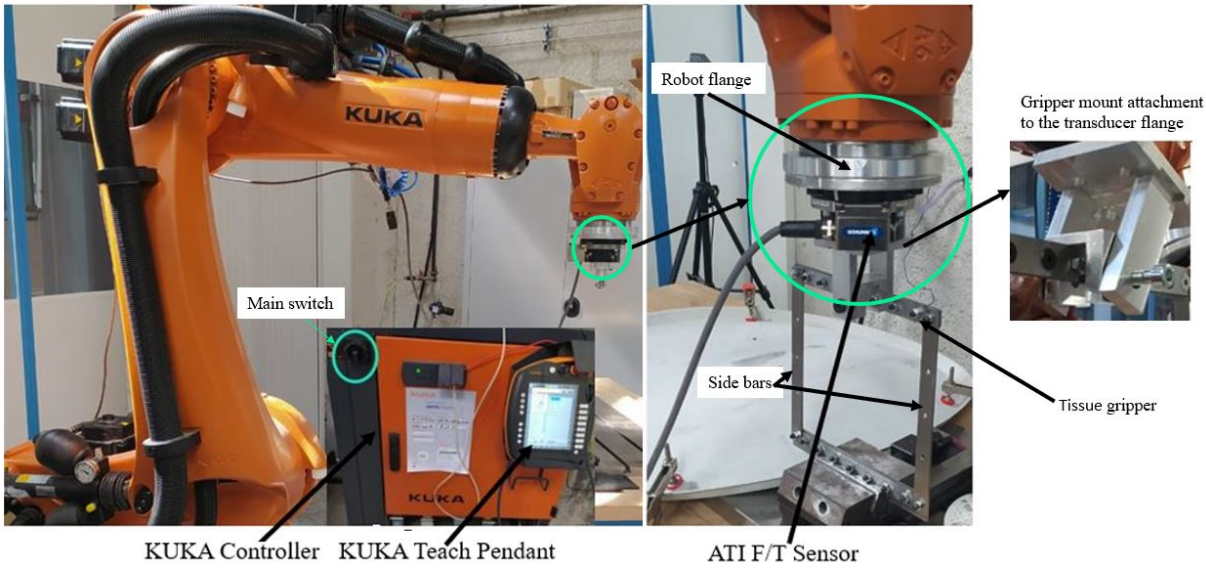

Fig. 3: Set-up apparatus.

A specific testing procedure Fig. 4, was conducted in setting up the fabric on the gripper mount, and finally on the KUKA robot platform. At first, several balanced plain weave samples were prepared. The rectangular shape test samples were of 100 mm by 200 mm in dimension. The test sample was set up and clamped onto the tissue gripper mount while ensuring that fibers were well-oriented, keeping the initial orthotropic nature of yarns in the weave. Once this was set, the gripper was mounted onto the robot's transducer flange and the bottom part clamped onto the metal base vice holder while keeping

the desired orientation in check. The gripper's side bars, which aid in reinforcing the structure to avoid deforming the fabric before testing, were removed leaving the fabric ready to undergo a simple mechanical test.

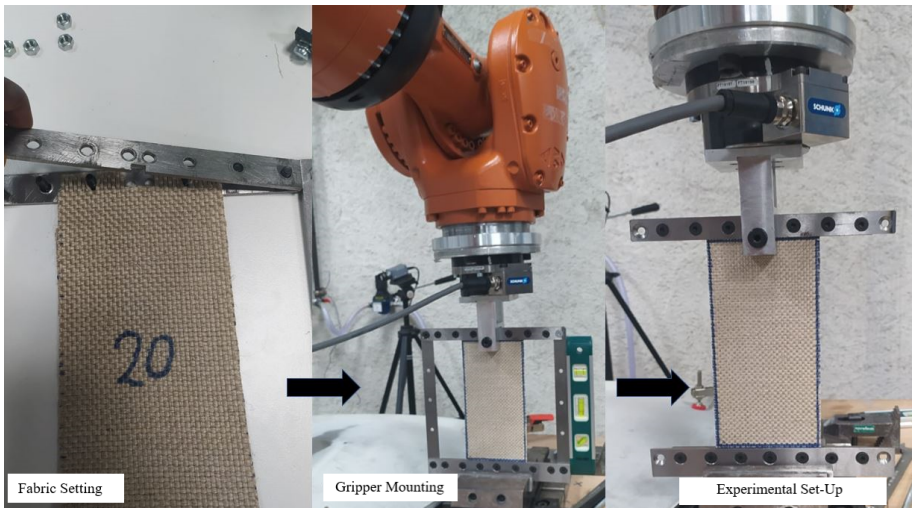

Fig. 4: Experimental Set-up Procedure.

A simple tensile test Fig. 5a was performed by applying a uniaxial tensile load. This was done by configuring a sensor-guided motion with the aid of KUKA RSI. The longitudinal displacement and the applied tension values were recorded and later analyzed to deduce the tensile characteristics of a plain weave textile. On the other hand, a tension-shear deformation mode Fig. 5b was also implemented experimentally by executing a superposition control mode. In this case, a constant uni-axial tensile force was kept while following a circular motion. The resulting tangential force (F_{sh}) was adopted as the shear force from the experiment. This force and the angle variation in the fiber direction were recorded and used in characterizing the fabric's shear behavior.

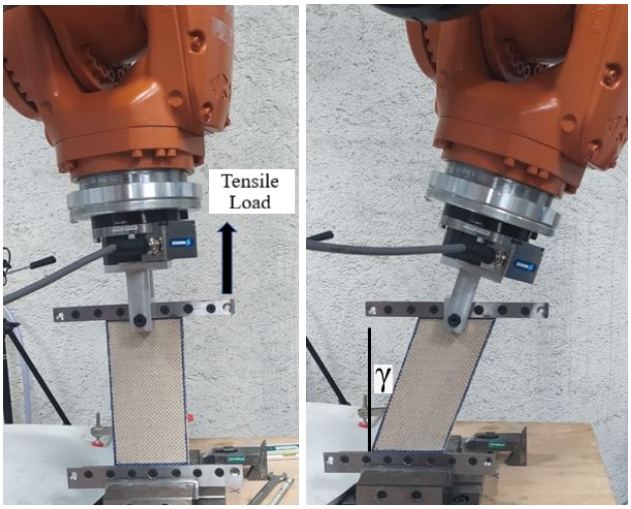

Tensile Deformation. Shear Deformation.

Fig. 5: Experimental Deformation Modes.

In the framework of data collection, the ATI network force/torque system provides EtherNet/IP and CAN bus communication interface which is compatible with standard Ethernet. This offers great functionality which enables the configuration of the ATI DAQ F/T sensor system, and in the same framework, the data was acquired, saved, and transferred to a personal computer for further analysis. The data of the forces, position, displacement, angles, and torques in the six-axis of the robot were obtained in a *.dat* format making it simple to read and post-process with the available numerical softwares.

Results and Discussions

Simulation Results. A constitutive anisotropic hyperelastic model was applied in the simulation of the potential strain energy density per unit area of the fabric to define the shear-tension coupling behavior. This aided in understanding the effect of coupling and justifying the fact that in practice, i.e during composite manufacturing, in-plane shear carries with it a component of the tensile load effect. A curve of shear strain energy vs angle (γ) was plotted and is presented in Fig. 6. The angle, in this case, represents the angular variations between yarns during the shear deformation mode given in percentages. In our case, we consider that, $\Delta\gamma \approx I_{sh}$.

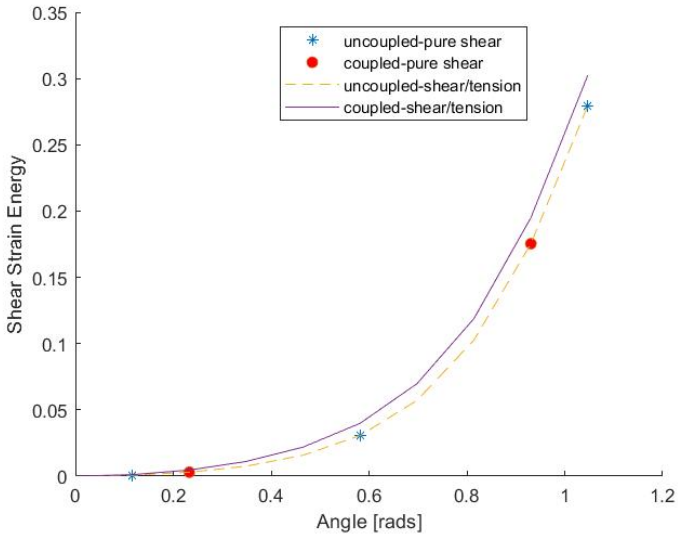

Fig. 6: Modeled shear-tension potential energy evolution curve.

As shown in Fig. 6, four characteristic curves of shear deformation mode were plotted under one graph. They are: (i) Uncoupled pure shear, (ii) Coupled pure shear, (iii) Uncoupled shear-tension, and (iv) Coupled shear-tension. The first three cases were superimposed altogether from the model data. This was due to the fact that equal shear energy strain density per unit volume of the fabric was recorded as a result of the uncoupling effect. Coupled pure shear without consideration of the tensile component contribution did not cause any significant change as is evident from the curve, whereas, coupled tension-shear recorded higher strain energy density. This implies that during forming, in-plane shear takes into account the tensile component.

Experimental Results: Uniaxial Tensile Loading. A tensile test was realized on a 100 mm by 200 mm sample of a balanced plain weave fabric, subjected to a uni-axial tensile force of up to 100 N. The experimental data for uni-axial tensile load and the displacement were collected and plotted as presented in Fig. 7. From this curve, two significant regions can be identified as described in [17, 19]. During the initial loading, a low stiffness region characterized by the non-linear part is observed. This represents the decrease in the yarn undulation also referred to as the decrimping phase. As the load increases further, the second region displays high stiffness where an increase in loading seems to be constant since at this point the fabric behaves then like a single loaded yarn. This leads to a fabric stretching phase which explains the near-linear rapid increase in the load-displacement curve. In considering that the load scales linearly according to the sample width, the load-displacement curve is transformed into a load per unit width-strain curve as shown in Fig. 8.

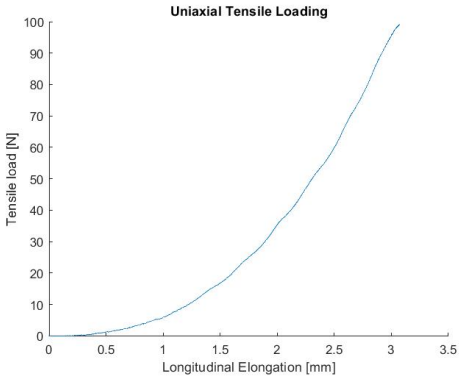

Fig. 7: The experimental tensile load-displacement curve.

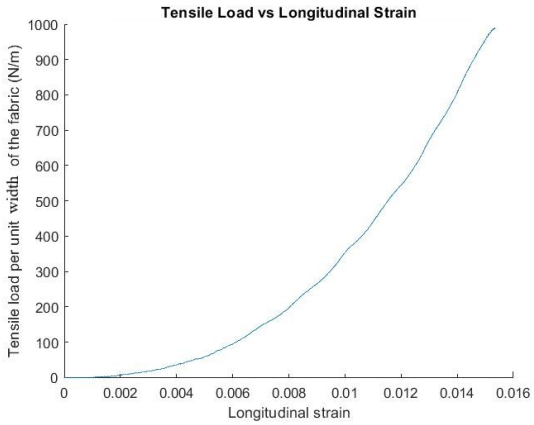

Fig. 8: Tensile load per unit width of the fabric against longitudinal/direct strain curve.

On the other hand, the elastic energy is stored in the fabric which implies that it scales according to the sample area. In this case, the load per unit width of the fabric is integrated over longitudinal elongation. We also noted that $\varepsilon = \lambda_{N1} - 1 = \sqrt{I4\alpha} - 1$ [11]. From this analysis, we obtained the tensile strain energy density versus $(I4 - 1)$ presented in Fig. 9 from which the model tension parameters could be identified according to Eq. 7.

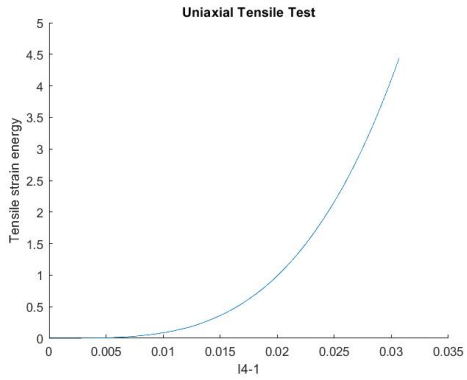

Fig. 9: Experimental tensile strain energy evolution.

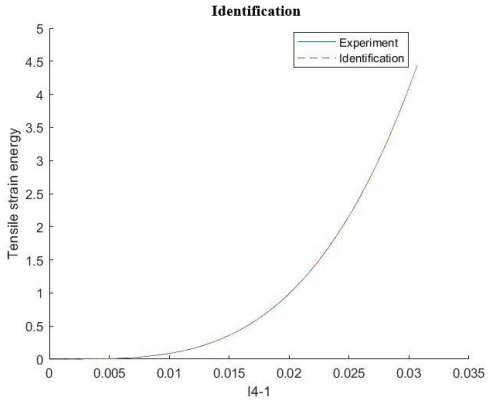

Fig. 10: Parameter identification through curve fitting.

Using the least square curve fitting optimization tool in Matlab software (*lsqcurvefit* command), the tensile strain energy density as a function of $(I4 - 1)$ curve was fitted to facilitate in parameter identification Fig. 10. The identified tension parameters are presented in Table 2

Table 2: Identified tension parameters of the flax plain weave fabric.

Tension Parameters [Pa]			
T_1	T_2	T_3	T_4
2033951.0533	109376.939	-613.1336	1.8133

Experimental Results: In-plane Shear Test. An in-plane shear behavior was measured experimentally using a KUKA robot. A rectangular-shaped fabric test sample with the initial yarn orientation of 90° was utilized in performing the shear test. The sample under a given constant tensile load was subjected to shearing with the loaded yarns following a circular trajectory. In fact, since the interest

is in the investigation of the coupling effect, the same results could be obtained by either applying different tension for a given shear or different shear for a given tension. Both approaches can be implemented using the robot. Several shear test experiments with the utilization of different test samples of the same material were conducted under different magnitudes of the yarn pre-tensions. The angular variations between yarns were recorded in steps of 5° to a final angle of 45°. The shear force (F_{sh}) which acted tangentially to the path trajectory was also recorded.
Measured force (F_{sh}) produces "work" as the tool center point of the fixture between the robot and the fabric rotates. Taking the sector length as L for a shear angle corresponding to $\gamma F \geq L = \gamma \cdot R$; where, R is the radius of the circular translation motion. Energy can be obtained from:

$$W_{sh} = \int_{L=0}^{L} F_{sh} \cdot dl = \int_{\gamma=0}^{\gamma F} F_{sh} \cdot (\gamma) \cdot R \cdot d\gamma \tag{11}$$

where dl represents an infinitesimal length along the trajectory, γ is the angle variation between yarns, and $d\gamma$ represents an infinitesimal angle.
Taking experimental results for the 20 N tension-shear tests, and utilizing the trapezoidal integration rule, the measured shear load was integrated cumulatively over shear angle in radians. The fabric area was computed and the resulting shear strain energy was obtained per unit area of the fabric. The evolution curve of shear strain energy per unit area of the fabric as a function of the shear invariant was plotted and presented in Fig. 11.

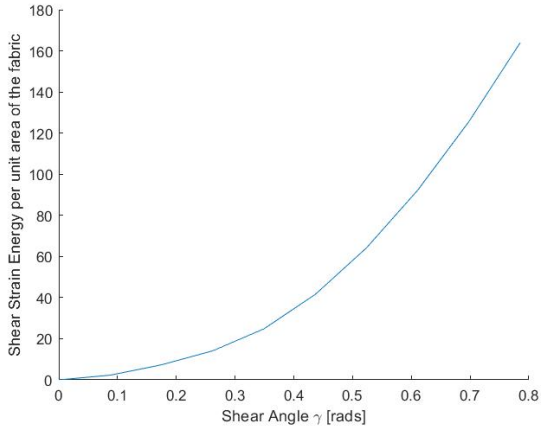

Fig. 11: Shear strain energy curve against the shear angle.

The coupled shear-tension hyperelastic constitutive model was fitted to the experimental data to identify both shear and coupling parameters while noting that $\Delta\gamma \approx I_{sh}$ [34]. Using Matlab software *fmincon* optimization solver with 'interior-point' algorithm, two experimental data sets from two different yarn pre-tensions, that is, at 20 N and 40 N were fitted simultaneously Fig. 12. The obtained parameters from the optimization procedure are presented in Table 3.

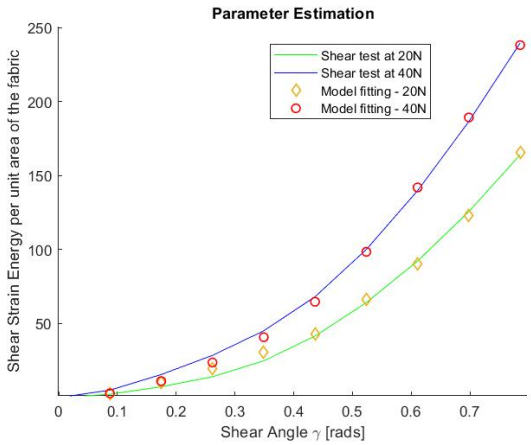

Fig. 12: Estimation of the model parameters / Identification.

Table 3: Identified shear and coupling parameters of the flax plain weave fabric.

Model Parameters [kPa]						
S_1	S_2	S_3	S_4	S_5	c_1	c_2
0.3825	-0.4331	5.9834	-11.5280	7.0785	-104670	6137500

Conclusions

A key interest in this research was to explore robotics' potential application in the study of mechanics of materials with the main aim of investigating the complex mechanical behavior of the technical textiles taking into account the effect of tension shear coupling.

A simple hyperelastic anisotropic, invariant-based constitutive model was formulated analytically, numerically, and presented in experimental deformation modes. The shear potential energy was considered with much emphasis to deduce the coupling behavior. This was implemented on a balanced plain weave fabric to characterize the non-linear behavior, strong anisotropy, together with the coupling effect contribution.

An experimental procedure was successfully implemented on the KUKA robot platform. A test gripper similar to the one used in the PFT test was fabricated and utilized in the characterization process. Trajectory path planning was generated with the aid of KUKA RSI while implementing position force control.

A simple mechanical test was performed on the test sample to validate the constituted model and identify the significant model parameters. The identification methods of tension, shear, and coupling parameters have been described and presented in detail.

The formulated model was fitted to the experimental shearing test results under uni-axial tensile mode. This resulted in a close fit to the tissue behavior showing that a constitutive model based on the continuum theory of mechanics can be used in describing the behavior of the fabrics and coupling mechanisms. Future research work will utilize this model to simulate the actual forming process.

Acknowledgements

This work was partially supported by the SIRYUS organization, by the ANR CODE-TRACK project (ANR-17-CE05-0014-01), by the ECOSYSPRO project, and by Campus France in Nairobi, Kenya.

References

[1] X. Q. Peng, Z. Y. Guo, and P. Harrison., A simple anisotropic fiber-reinforced hyperelastic constitutive model for woven composite fabrics, Int. J. Mater. Form. 3(1) (2010) 723-726.

[2] A. Charmetant, J.C. Orliac, E. Vidal-Sallé, P. Boisse, Hyperelastic model for large deformation analyses of 3D interlock composite preforms, Comp. Sci. and Tech. 72(12) (2012) 1352-1360.

[3] T.K. Das, P. Ghosh, and N.C. Das, Preparation, development, outcomes, and application versatility of carbon fiber-based polymer composites: a review, Adv. Compos. Hybrid. Mater. 2(2) (2019) 214–233.

[4] M. Hann, Textile Design: Products and Processes, CRC Press, United States, 2020.

[5] K. Buet-Gautier, P. Boisse, Experimental analysis and modeling of biaxial mechanical behavior of woven composite reinforcements, Exp. Mecha. 41(3) (2001) 260-269.

[6] P. Boisse, N. Hamila, E. Vidal-Sallé, F. Dumont, Simulation of wrinkling during textile composite reinforcement forming. Influence of tensile, in-plane shear and bending stiffnesses, Compos. Sci. Technol. 71(5) (2011) 683-692.

[7] M.A. Turk, B. Vermes, A.J. Thompson, J.P.-H. Belnoue, S.R. Hallett, D.S. Ivanov, Mitigating forming defects by local modification of dry preforms, Compos., Part A Appl. sci. manuf. 128 (2020).

[8] S. Mathieu, N. Hamila, F. Bouillon, P. Boisse, Enhanced modeling of 3D composite preform deformations taking into account local fiber bending stiffness, Compos. Sci. Technol. 117 (2015) 322-333.

[9] F. Nosrat-Nezami, T. Gereke, C. Eberdt, C. Cherif, Characterisation of the shear–tension coupling of carbon-fibre fabric under controlled membrane tensions for precise simulative predictions of industrial preforming processes, Compos., Part A Appl. sci. manuf. 67 (2014) 131-139.

[10] M.J. King, P. Jearanaisilawong, S. Socrate, A continuum constitutive model for the mechanical behavior of woven fabrics, Int J Solids Struct 42(13) (2005) 3867-3896.

[11] X. Peng, Z. Guo, T. Du, W.-R. Yu, A simple anisotropic hyperelastic constitutive model for textile fabrics with application to forming simulation, Compos. B. Eng. 52 (2013) 275-281.

[12] E. De Luycker, F. Morestin, P. Boisse, D. Marsal, Simulation of 3D interlock composite preforming, Compos. Struct. 88(4) (2009) 615-623.

[13] M. Komeili, A. S. Milani, On effect of shear-tension coupling in forming simulation of woven fabric reinforcements, Compos. B. Eng. 99 (2016) 17-29.

[14] P. Badel, E. Vidal-Sallé, P. Boisse, Computational determination of in-plane shear mechanical behaviour of textile composite reinforcements, Comput. Mater. Sci. 40(4) (2007) 439-448.

[15] Y. Aimène, E. Vidal-Sallé, B. Hagège, F. Sidoroff, P. Boisse, A hyperelastic approach for composite reinforcement large deformation analysis, J. Compos. Mater. 44(1) (2010) 5-26.

[16] E. Syerko, C. Sébastien, C. Binetruy, Models for shear properties/behavior of dry fibrous materials at various scales: a review, Int. J. Mater. Form. 8(1) (2015) 1-23.

[17] H.O. Werner, F. Schäfer, F. Henning, L. Kärger, Material Modelling of Fabric Deformation in Forming Simulation of Fiber-Metal Laminates–A Review on Modelling Fabric Coupling Mechanisms, 24th International Conference on Material Forming, Liège, Belgique. (2021).

[18] J. Launay, G. Hivet, A. V. Duong, P. Boisse, Experimental analysis of the influence of tensions on in plane shear behaviour of woven composite reinforcements, Compos. Sci. Technol. 68(2) (2008) 506-515.

[19] M. Haghi Kashani, A. Rashidi, B.J. Crawford, A.S. Milani, Analysis of a two-way tension-shear coupling in woven fabrics under combined loading tests: Global to local transformation of non-orthogonal normalized forces and displacements, Compos., Part A Appl. sci. manuf. 88 (2016) 272-285.

[20] P. Boisse, J. Colmars, N. Hamila, N. Naouar, Q. Steer, Bending and wrinkling of composite fiber preforms and prepregs. A review and new developments in the draping simulations, Compos. B. Eng. 141 (2018) 234-249.

[21] L. Kärger, A. Bernath, F. Fritz, S. Galkin, D. Magagnato, A. Oeckerath, A. Schön, F. Henning, Development and validation of a CAE chain for unidirectional fibre reinforced composite components, Compos. Struct. 132 (2015) 350-358.

[22] P. Harrison, F. Abdiwi, Z. Guo, P. Potluri, W.R. Yu,, Characterising the shear–tension coupling and wrinkling behaviour of woven engineering fabrics, Compos., Part A Appl. sci. manuf. 43(6) (2012) 903-914.

[23] Y. Yao, X. Huang, X. Peng, P. Liu, G. Youkun, An anisotropic hyperelastic constitutive model for plain weave fabric considering biaxial tension coupling, Text. Res. J. 89(3) (2019) 434-444.

[24] P. Harrison, Normalisation of biaxial bias extension test results considering shear tension coupling, Compos., Part A Appl. sci. manuf. 43(9) (2012) 1546-1554.

[25] A.J.M. Spencer (Ed), Continuum theory of the mechanics of fibre-reinforced composites, Springer-Verlag, New York. 282 (1984) 1-32.

[26] X. Peng, Z. Guo, T. Du, W.-R. Yu, A simple anisotropic hyperelastic constitutive model for textile fabrics with application to forming simulation, Compos. B. Eng. 52 (2013) 275-281.

[27] I. Taha, Y. Abdin, S. Ebeid, Comparison of picture frame and Bias-Extension tests for the characterization of shear behaviour in natural fibre woven fabrics, Fibers and Polymers 14(2) (2013) 338-344.

[28] P. Harrison, M.J. Clifford, A.C. Long, Shear characterisation of viscous woven textile composites: a comparison between picture frame and bias extension experiments, Compos. Sci. Technol. 64(10-11) (2004) 1453-1465.

[29] C. Krogh, K.D. White, A. Sabato, J.A. Sherwood, Picture-frame testing of woven prepreg fabric: an investigation of sample geometry and shear angle acquisition, Int. J. Mater. Form.. 13(3) (2020) 341-353.

[30] J. Cao, R. Akkerman, P. Boisse, J. Chen, H.S. Cheng, E.F. de Graaf, J.L. Gorczyca, P. Harrison, G. Hivet, J. Launay, W. Lee, L. Liu, S.V. Lomov, A. Long, E. de Luycker, F. Morestin, J. Padvoiskis, X.Q. Peng, J. Sherwood, Tz. Stoilova, X.M. Tao, I. Verpoest, A. Willems, J. Wiggers, T.X. Yu, B. Zhu, Characterization of mechanical behavior of woven fabrics: Experimental methods and benchmark results, Compos., Part A Appl. sci. manuf. 39(6) (2008) 1037-1053.

[31] S.V. Lomov, Ph. Boisse, E. Deluycker, F. Morestin, K. Vanclooster, D. Vandepitte, I. Verpoest, A. Willems, Full-field strain measurements in textile deformability studies, Compos., Part A Appl. sci. manuf. 39(8) (2008) 1232-1244.

[32] B. Siciliano, L. Sciavicco, L. Villani, G. Oriolo, Robotics: modelling, planning and control, Advanced Textbooks in Control and Signal Processing, Springer 2009.

[33] J. Schrimpf, Automated sewing using conveyor belts, 2016 IEEE 21st International Conference on Emerging Technologies and Factory Automation (ETFA) (2016) 1-4.

[34] Y. Yao, X. Huang, X. Peng, Y. Gong, An anisotropic constitutive model with biaxial-tension coupling for woven composite reinforcements, ESAFORM 2016 AIP Conference Proceedings. 1769(1) (2016) 170006.